University of North Carolina Asheville
Journal of Undergraduate Research
Asheville, North Carolina
May 2019

Synthesis and Antibacterial Evaluation of Empetroxepin A and B and Related Analogs

Marcia Thacher
Chemistry
The University of North Carolina Asheville
One University Heights
Asheville, North Carolina 28804 USA

Faculty Advisor: Dr. Amanda Wolfe

Abstract

The World Health Organization recognizes antimicrobial resistance as a global problem caused by the decreasing effectiveness of conventional antibacterial drugs. Estimates are that by 2050, 10 million lives a year would be at risk from drug-resistant infections. The Wolfe research group works to develop novel antibiotics through the isolation, extraction, and characterization of secondary metabolites produced by bacteria, and by leveraging antibiotic scaffolds provided by nature to synthesize and optimize antibacterial activity through medicinal chemistry techniques. Empetroxepin A and B, isolated from the black crowberry tree, *Empetrum nigrum L.* (*Ericaceae*), exhibited weak antimycobacterial activity against *M. tuberculosis* H37Ra (MIC = 100 µg/mL, IC50 =25.7 µg/mL and IC50 = 28.5 µg/mL) and selectivity against human embryonic kidney 293 cells (IC50 45.6 µg/mL and IC50 96.7 µg/mL). Prior research resulted in a synthetic strategy for both empetroxepin analogs by forming an alkene bridge between a triphenylphosphate salt and a trimethylsilane (TMS) protected salicylaldehyde followed by cyclization using potassium carbonate and a copper oxide catalyst. This research introduced an alternate strategy using an Ullman type reaction for cyclization and transfer hydrogenation to reduce an aromatic alkene, increasing overall yields from 0.5% to over 13%. The effects of new ligands on the empetroxepin core were investigated by introducing commercially available substituted salicylaldehydes chosen for their influence on steric and electrochemical properties. Results revealed deprotected analogs to have cell death activity against Gram-positive *S. aureus* (0.46 to 0.92 mg/mL) but not Gram-negative *E. coli* bacteria. Cell wall viability assays revealed broad spectrum activity, indicating empetroxepin acts to inhibit bacterial cell walls and that activity was significantly affected by substituent type and position.

1. Introduction

Increasing antimicrobial resistance is a global problem caused by the decreasing effectiveness of conventional microbial drugs due to overuse and misuse of antimicrobial agents.[1] O'Neill and coauthors published a report commissioned by the British government, estimating that by 2050, 10 million lives a year would be at risk from the rise of drug-resistant infections, which equates to 1 person dying every 3 seconds from lack of antibiotic availability.[2] Already, more people die of methicillin-resistant *Staphylococcus aureus* (MRSA) infection in US hospitals than of HIV/AIDS and tuberculosis combined[3], and a total of 700,000 lives are lost worldwide attributable to antibiotic resistance. If predictions are realized, Figure 1 illustrates that antibiotic resistance will eclipse cancer as the number two global killer.[2]

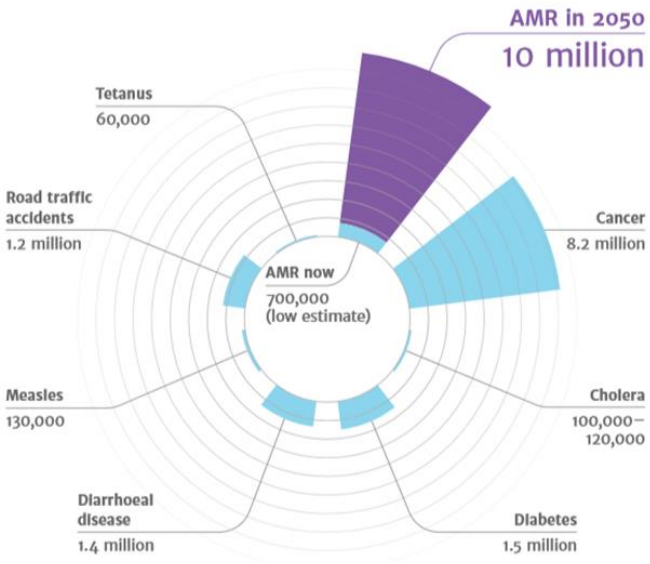

Figure 1. Projected antimicrobial resistance deaths.

Figure 1 Deaths annually attributable to antimicrobial resistance as compared to other causes. (Graphic used in accordance with the terms of the Creative Commons Attribution 4.0 International Public License.)

After the "Golden Age" of antibiotic discovery from the 1940s to 1960s led to the discovery of nearly all antibiotic classes in use today[4], a combination of factors led to a void in the number of new antibiotic discoveries for bacterial infections (Figure 2). These factors ranged from a changing regulatory environment, to increased drug safety standards, as well as failure of modern drug discovery techniques such a high throughput screening.[5] The number of new treatments approved for bacterial infections has decreased from an average of four new drugs per year in the 1980s to now less than one annually. Due to this dearth of new antibiotics, clinicians have been noted to use previously discarded drugs, such as colistin, associated with significant toxicity because of extreme limitations in antibiotic options.[3]

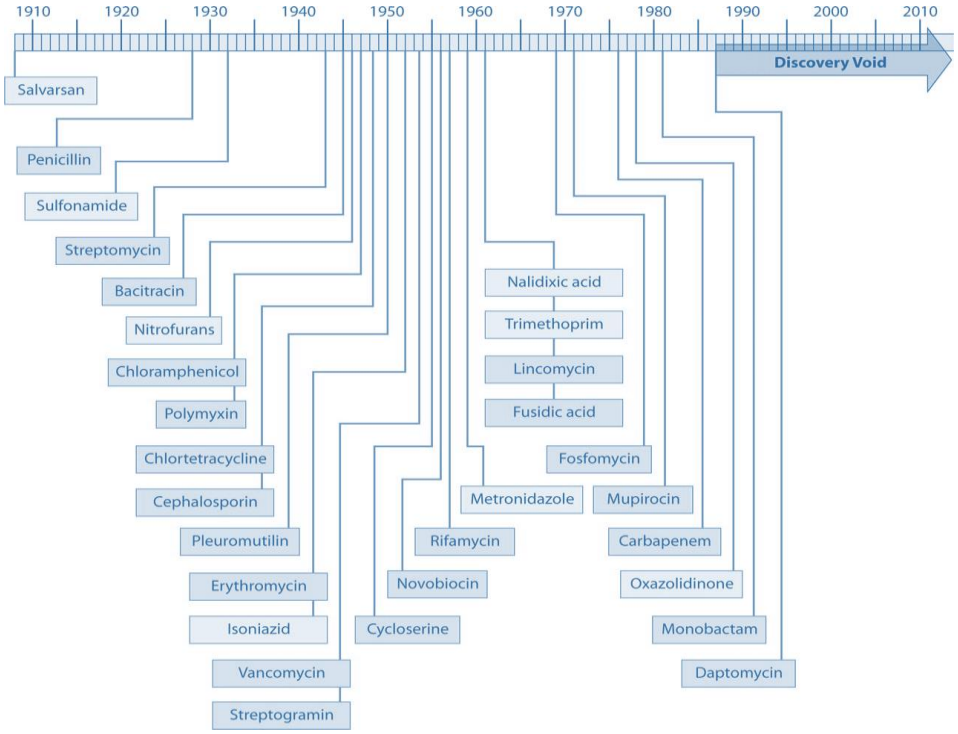

Figure 2. Antibacterial drug discovery dates.

Figure 2 Dates indicated are those of reported initial discovery or patent. (Graphic used with permission of the American Society for Microbiology, Copyright © 2011.)

Antibacterial resistance occurs when one or more members of a bacterial population survive exposure to an antibiotic. When an antibiotic is administered, these survivors can then proliferate unhindered and pass to their offspring the same genes that made them resistant. In some cases, bacteria can even donate their antibacterial resistance capability to other bacteria, further increasing resistance. This resistance often requires a larger antibiotic concentration or a different drug altogether to address the same bacterial infection during future treatments. Ultimately, this can be dangerous because antibiotics are not entirely selective to the target bacteria, and during administration, can cause the death of good bacteria in the body. Successfully treating infections in an environment of constantly evolving resistance requires steady development of a new arsenal of drugs.

Among the most problematic antibacterial resistant strains are the Gram-positive bacteria, MRSA[7], and the multidrug-resistant (MDR) *Mycobacterium tuberculosis*. Additionally, data from the Centers for Disease Control and Prevention (CDC) show rapidly increasing rates of infection due to Gram-positive vancomycin-resistant *Enterococcus faecium* (VRE), and fluoroquinolone-resistant *Pseudomonas aeruginosa* (FRPA) which is Gram-negative.[3] The incidence of resistant strains of MRSA, VRE, and FRPA are shown in Figure 3 compared against the reducing number of new treatments available. MRSA, VREs, and FRPA are concerning for hospital-borne infections acquired during surgeries or other treatments and can affect those with compromised immune systems such as HIV/AIDS patients and the elderly.[6]

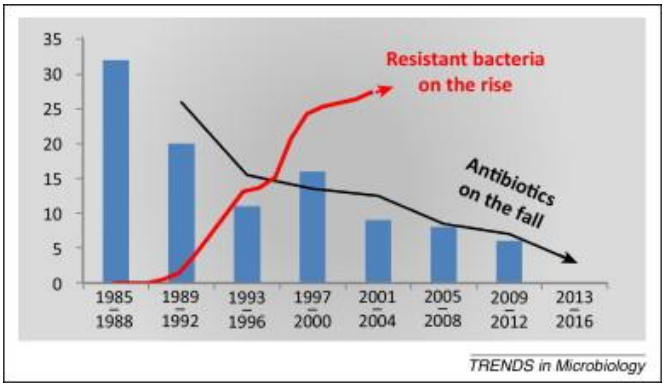

Figure *3*. Trends in Antibiotic Development and Resistance. (Reprinted from Trends in Microbiology Copyright 2014 with permission from Elsevier.)

The call from organizations such as the Infectious Disease Society of America and the World Health Organization to address the growing issue of antibacterial resistance and the antibiotic void, is being answered by laboratories such as Dr. Amanda Wolfe's at the University of North Carolina Asheville. The Wolfe research group works to develop novel antibiotics through the isolation, extraction, and characterization of secondary metabolites produced by bacteria, and by leveraging antibiotic scaffolds provided by nature to synthesize and optimize antibacterial activity through medicinal chemistry techniques. In 2017, the Wolfe Laboratory announced the isolation of pseudopyronine B, a pseudomonas species active against *Staphylococcus aureus* (IC_{50} = 0.1 µg/mL). Laboratory synthesis of the compound and its analogs enabled structure activity relation (SAR) evaluations, revealing a direct relationship between antibacterial activity and C3/C6 alkyl chain length.[9] Similar analyses have targeted compounds such as pestalone and depsidones (Figure 4).

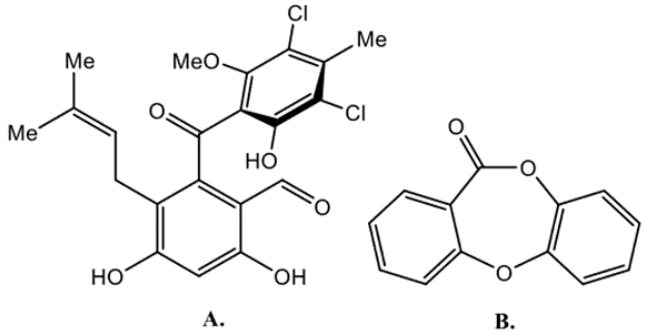

Figure 4. Target molecules studied by the UNC Asheville medicinal chemistry research group: pestalone (A) and depsidone (B).

Erin Young, a prior member of Dr. Wolfe's research group, initiated investigation into empetroxepin A and B (Figure 5) as target lead compounds in the development of a novel antibacterial drug. Empetroxepin A and B, isolated from the black crowberry tree, *Empetrum nigrum L.* (*Ericaceae*), exhibited weak antimycobacterial activity against *M. tuberculosis* H37Ra (MIC = 100 µg/mL, IC_{50} =25.7 µg/mL and IC_{50} = 28.5 µg/mL) and selectivity against human embryonic kidney 293 cells (IC_{50} 45.6 µg/mL and IC_{50} 96.7 µg/mL).[10] However, sufficient structural similarities exist with known bioactive molecules such as depsidone, flavin, and chalcone, suggesting that activity might be enhanced through modifications to the empetroxepin core. Erin concluded her investigations with a synthetic strategy to access the core of empetroxepin.

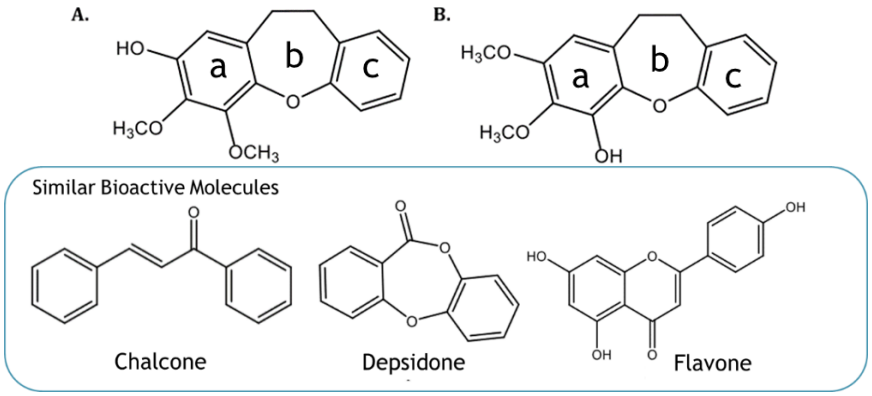

Figure 5. Comparison of empetroxepin to other antibacterial compounds. (Top) Structures A and B of empetroxepin, a novel dibenze[b,f]oxepin compound. Rings a, b, and c are labeled for reference. (Bottom) Molecules with antibacterial properties and similar structure to empetroxepin.

The prior synthesis of empetroxepin developed in the Wolfe Laboratory, shown in Figure 6, follows a three-phase strategy. First, the formation of the triphenylphosphate salt **4** is carried out using 1 equivalent of triphenylphosphine (PPh_3) in DMF with a 99% yield. Next, an alkene bridge is formed through a Wittig olefination of the triphenylphosphate salt **4** and trimethylsilane (TMS) protected salicylaldehyde **5** with an 91% yield, 36% cis and 63% trans. The aldehyde is protected using pyridine (2.5 eq) and TMS-Cl (2.1 eq) in anhydrous dichloromethane (DCM). Finally, cyclization to form the ether bridge is achieved using potassium carbonate and a copper oxide catalyst in anhydrous pyridine with a 19% yield. Hydrogenation of the alkene bridge using activated palladium on carbon and hydrogen gas in anhydrous ethyl acetate (EtOAc) were proposed to form the empetroxepin isomers **9a** and **9b**.

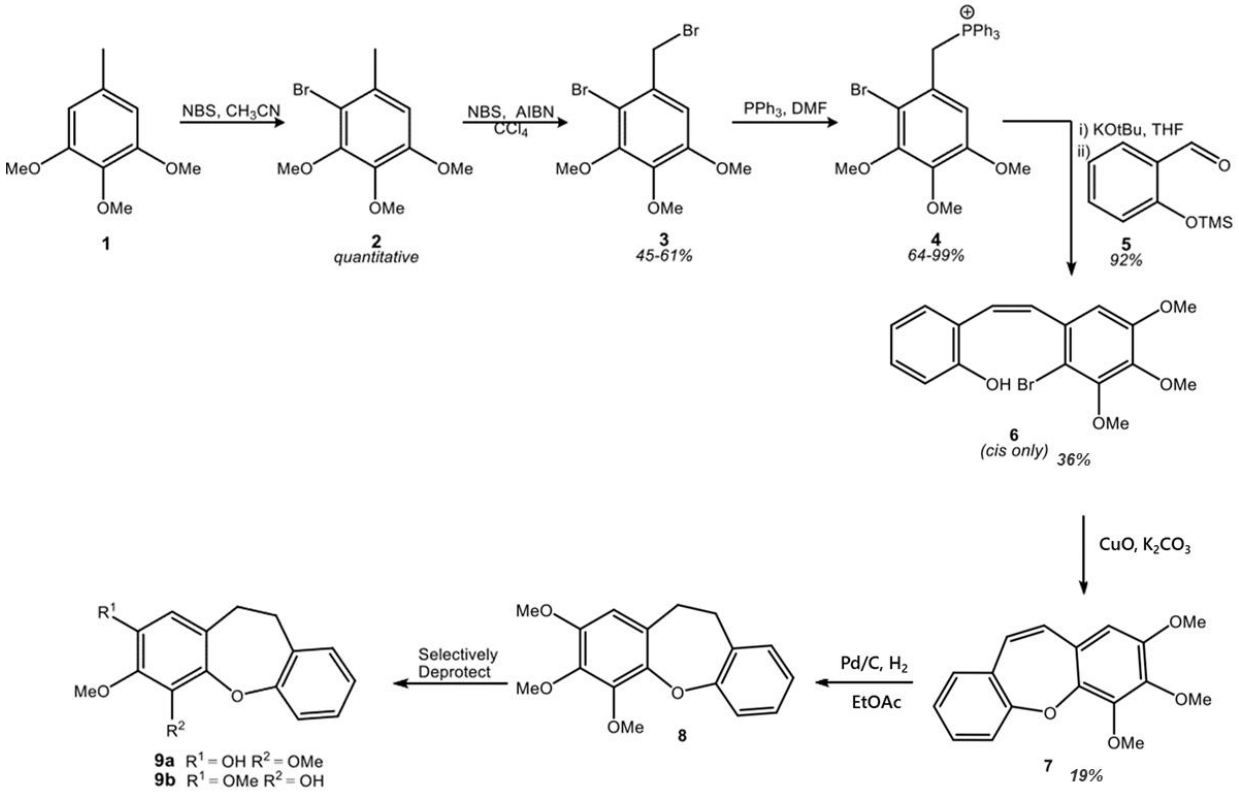

Figure 6. Original proposed synthesis of empetroxepins A and B.

The goal of improving the bioactivity of empetroxepin hinges upon the existing synthesis strategy, specifically focusing on the Wittig olefination between compounds **4** and **5**. Since substitutions already exist on the A ring in the natural empetroxepin A and B compounds, the focus for this project is to make substitutions on the outer C ring. By changing the aromatic ring substitutions on compound **5** prior to its role as a reagent in the formation of the alkene bridge, the substitutions can be carried over to the final product with only minor changes in the remaining synthesis steps. However, while complete, the synthesis yielded less than 0.5% for the hydrogenation reaction, and neither the hydrogenated product nor the final deprotected empetroxepin analogs were ever successfully characterized. Thus, the baseline synthesis strategy required modification prior to pursuing analogs.

Initial assays against *M. tuberculosis* H37Ra of empetroxepin A and B and other isolated dibenze(b,f)- oxepins offer some insight into the effect of substitutions. As shown in Figure 7, isolated extracts from *Bauhinia purpurea* with the same 6,7,6 tricyclic core as empetroxepin but different arrangements of hydroxy and methoxy substituents, showed that in general, para substituted ketones on the A ring at C1 and C4 improved activity from MIC 183.8 µM to 87.4 µM, but was negatively influenced by a hydroxy substituent on the opposite ring (MIC 24.4 µM to 87.4 µM and 174.8 µM). While activity was reduced by the presence of a hydroxy on the C ring, a two-fold improvement resulted when moved from C8 from C7 (87.4 µM MIC to 174.8 µM).[11] Similar to findings by the empetroxepin discovery team, swapping the position of the methoxy and hydroxy on ring A had little effect.[10] However, the addition of a hydroxy or methoxy at C4 significantly reduced antimycobacterial activity from MIC 183.8 µM to 331.1 µM and 662.2 µM, respectively.

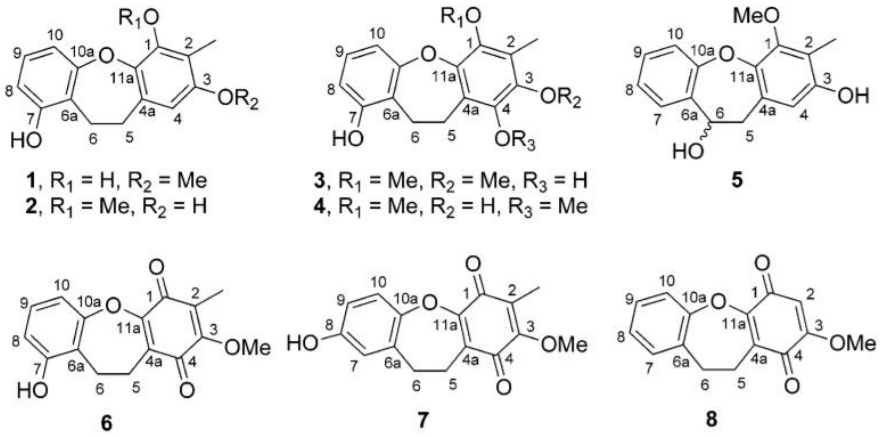

Figure 7. Isolated dibenze(b,f)- oxepins from *B. purpurea*. (Reprinted with permission from the Journal of Natural Products, Copyright 2007 American Chemical Society.)

A literature survey of active antibacterial compounds and reported structure activity relationships determined which analogs to pursue in the empetroxepin evaluations. In a novel method to reverse engineer bedaquiline, the first new tuberculosis drug in forty years to be approved by the FDA, each of its individual constituents was assessed for its contribution to the efficacy of the drug and its analogs were synthesized to evaluate less complex versions. Compared to a baseline in vitro performance of MIC = 0.06 µg/mL against *M. tuberculosis*, several new analogs were discovered that had MIC = <0.5 µg/mL. Bedaquiline optimization highlighted that all successful analogs shared a dimethyl amino group of maximum two carbon length. A second observation was that analogs with piperazine retained activity but through a different mechanism than the original bedaquiline.[12] These findings suggest that terminal amino groups and piperazine should also be explored in analogs of empetroxepin.

A recently isolated pseudopyronine B compound was found to have antibacterial activity against *S. aureus* and *B. subtilis* at levels of IC_{50} of 0.1 mg/mL and 0.3 mg/mL, respectively.[9] Hydrocarbon chain substitutions at positions C3/6 showed a direct correlation of chain length to antibiotic activity. Tests showed that shorter side chains were more active against *E. coli*, whereas longer side chains up to five carbons were more active against gram-positive *S. aureus* and *B. subtilis.* Thus, lipophilic and/or steric character of the molecule can influence its antibiotic activity and are worthy of evaluation with empetroxepin.

A subset of depsidones called spiromastixones have hydrocarbon chain substitutions on the outer rings in addition to varying combinations of hydroxy and chlorines. Depsidones are like empetroxepin in that both exhibit a tricyclic molecule with a 7-membered center ring, however, depsidones contain an additional ester group in the center ring.

As the number of depsidone chlorine atoms increases, the antibiotic activity increases. Additionally, an aldehyde replacement for a methoxy improves activity.[13] The close similarity of depsidones and empetroxepin indicates chlorine and methoxy groups could have a similar effect in analogs.

This work capitalized on prior findings from across the research community to direct electronic and steric substitutions onto ring C of the empetroxepin molecule. Figure 8 shows the functional groups used to generate a first-pass assessment of antibacterial activity. Each empetroxepin analog was tested for antibacterial activity against a panel of Gram-positive (*S. aureus*) and Gram-negative (*E. coli*) bacteria. Analogs exhibiting significant antibiotic activity, levels below 1 µg/mL, were evaluated for their antibiotic mechanism of action.

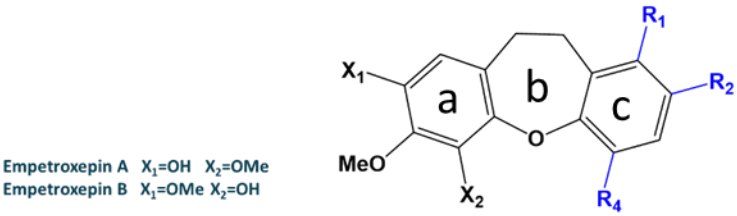

	Position	Electronegativity	Steric	Other
Targeted Analogs	$-R_1$ (Cl only)	-Cl	$-CH_3$	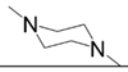
		-Br	$-CH_2CH_3$	
	$-R_2$	-OH	$-C(CH_3)_3$	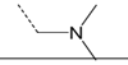
	$-R_4$ (Cl only)	$-NH_2$	-H	$-OCH_3$

Figure 8. Substitutions to empetroxepin ring c.

2. **Results and Discussion**

2.1. Synthesis Strategy

Replication of the synthesis set forth by Young, et. al. was first necessary to demonstrate feasibility and to obtain enough product for both antibacterial assays and a baseline comparison against the new analogs. The original synthesis of empetroxepin A and B is shown in Figure 6. While complete, the synthesis yielded less than 0.5% for the hydrogenation reaction and neither the hydrogenated product nor the final deprotected empetroxepin analogs were ever successfully characterized. Therefore, the existing synthesis strategy could not be applied to the formation of empetroxepin analogs and first required modification to increase overall yields.

Two issues with the initial synthesis strategy contributed to the low yields. First, alkene reduction of the central ring proved especially difficult due to conjugation with the two outer benzene rings. In the complete synthesis of bulbophylol, Lin, et al. discovered that the high temperatures required for the palladium catalyzed hydrogenation to be successful, resulted in the loss of the bromine needed for ring closure. They explored alternative reducing agents such as Zn/HCl and $NaBH_4/NiCl_2$ and found transfer hydrogenation using TsNHNH2/NaOAc to be the most successful.[14] The success of transfer hydrogenation with empetroxepin analogs is demonstrated by increases in yield from 0.5% in the initial empetroxepin hydrogenation strategy to 36% using transfer hydrogenation.

A second contributor to the low yields in the originally proposed synthesis strategy was the ring closure reaction. Initial reported yields were high, but only because they benefited from the correct cis alignment of the Br and hydroxy for the Ullman reaction. Introduction of transfer hydrogenation allowed retention of both the cis and trans isomer products in reaction 4, leading to an immediate increase in yields from 33% to 91% for product 6. Negating the need to use only cis product for ring closure, hydrogenation was performed before ring closure, resulting in an overall yield increase of product 8 from negligible to 8%. The final overall synthesis strategy used to produce analogs is shown in Figure 9.

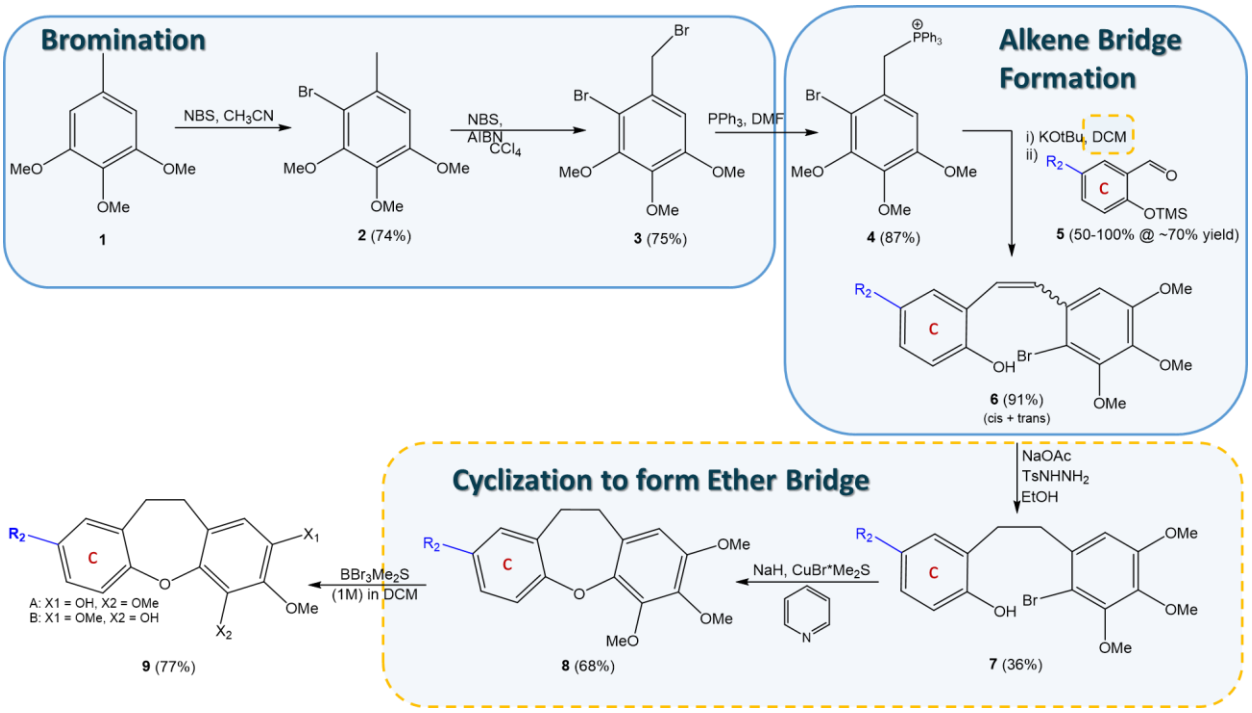

Figure 9. Empetroxepin analog synthesis strategy.

Figure 9. Final synthesis strategy applied to produce empetroxepin analogs. Modifications to the original synthesis strategy are denoted by dashed orange lines. The order of ring closure and hydrogenation is reverse of the original synthesis.

While not a contributor to the low yields in the original synthesis strategy, it was also discovered that some TMS protected substituted salicylaldehydes are especially prone to decomposition, most notably the chlorine analog. Even under vacuum conditions, TMS protection was lost as observed via H^1 NMR analysis of time sequenced samples during evaporation of the THF solvent in vacuo. To address decomposition, the solvent was switched to DCM such that the TMS protected salicylaldehydes could remain in solution and moved directly to the Wittig olefination reaction which also uses DCM as the solvent. It is believed that THF and DCM would produce comparable yields but was not verified. Leaving product in solution prevented further product characterization and yield calculations for TMS protection reactions, therefore were simply combined into the Wittig olefination where noted in reaction conditions. Analogs synthesized prior to implementing this change have notably low (~30%) Wittig reaction yields as compared to later analogs (~60%). A final general mention about TMS protection, is that due to its sensitivity to water, it is recommended to only condense in vacuo and store product under inert conditions. This team experienced significant decomposition of product when the weather changed from winter to spring, leading to higher atmospheric moisture levels.

The analogs expected to be the most challenging to synthesize were those with highly electronegative atoms. Hence, due to excess available material, the extreme case of 2,4-dichloro-salicylaldehyde served to demonstrate feasibility of the synthesis strategy for ring C substitutions. The two additional electronegative chlorine molecules were expected to reduce the reactivity of the aldehyde functional group, making formation of the alkene bridge from the ylide and substituted benzaldehyde more challenging. However, the increase in acidity of the alcohol was predicted to improve the TMS protection reaction.

As expected, the initial Wittig olefination with 2,4-dichloro-salicylaldehyde following room temperature reaction conditions, as was applied with the non-substituted benzaldehyde, yielded insufficient product to be characterized. The same reagents under reflux conditions resulted in an 8% higher yield than the unsubstituted product, indicating that aldehyde bridge formation with inductive electron withdrawing groups would have a higher activation energy but could be overcome through the addition of heat. Reflux conditions were then introduced for analogs with electronegative atoms. The TMS protection step also behaved as predicted and, as demonstrated via H^1 NMR, yielded 100% of the protected alcohol whereas only 66% of the non-substituted salicylaldehyde was protected. It is noted that

2,4-dichloro-salicylaldehyde TMS protection results were during low moisture atmospheric conditions and minimal time lapse between TMS protection and Wittig olefination. Evaluations with 2,4-dichloro-salicylaldehyde were then concluded since hydrogenation and ring closure reactions were expected to perform similarly to those without electronegative atoms. Reaction yields for each analog are shown in Table 1. To date, only analogs with percent yield for products 8 and 9 in table 1 have been synthesized.

Published reaction conditions for the deprotection of alcohols from methoxy functional groups suggest reflux above 40 ºC. In order to selectively control for deprotection, lower temperatures from room temperature to 30 ºC were evaluated. Temperatures below 20 ºC allowed for detection of single, dual, or triple deprotected analogs, however the position of deprotection was somewhat random and isolates contained mixed product. To proceed with antibacterial assays, all hydroxy groups were deprotected using the original 40 ºC reflux conditions.

Table 1. Empetroxepin Analogs Synthesized with Percent Yields

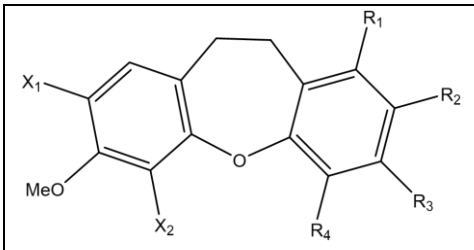

Empetroxepin A X_1=OH X_2=OMe
Empetroxepin B X_1=OMe X_2=OH

Analog		Substituents			Percent Yield by Product			
		R1	R2	R4	6	7	8	9
1	Unsubstituted	-	-	-	73	35	62	-
2	2,4 dichloro				25	-	-	-
2	2-chloro	-	Cl	-	91	50	68	77
3	1-chloro	Cl	-	-	69	73	82	22
4	4-chloro	-	-	Cl	56	54	8.5	26
5	2-bromo	-	Br	-	59	77	61	25
6	2-hydroxy	-	OH	-	87	66	25	-
7	2-methoxy	-	OCH_3	-				64
8	2-methyl	-	CH_3	-	67	76	71	68
9	2-ethyl	-	CH_2CH_3	-	-	-	trace	-
10	2-t-butyl	-	C(CH3)3	-	-	-	-	-
11	2-amine	-	NH_2	-	41 (nitro)	66	21	-
12	2-piperazine	-	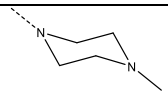	-	-	-	trace	-
13	2-dimethylamine	-		-	-	-	trace	-

2.2. Antibacterial Assays

To observe the effects of both substitutions to empetroxepin ring C and the antibacterial activity contribution of the unmodified A ring, cell death assays against *S. aureus* and *E. coli* were performed with protected and deprotected analogs. Cell death was performed on all protected analogs but only the protected analogs with methyl and chlorine in position R_2, and the chlorine in position R_4 were assayed. None of the protected analogs exhibited cell death activity at the highest concentration of 1000 µg/mL against *S. aureus* or *E. coli*. However, all three deprotected analogs did exhibit cell death activity against *S. aureus* as shown in Table 2, but not against *E. Coli*. Chlorine in position R_4 had the lowest IC_{50} value at 0.46 mg/mL, slightly lower than chlorine in position R_2. Both chlorine analogs performed better either the methyl substituted analog or R_2 substituted chlorine analog. Results indicate that molecular interactions with the hydroxyl groups on empetroxepin A ring contribute to cell death activity against *S. aureus* and that substituent position also has an effect.

Table 2. Empetroxepin analog IC_{50} values against *S. aureus*

Analog	Substituent (position)	IC_{50} (mg/mL)
Protected	Cl (R_4)	0.46
	Cl (R_2)	0.57
	CH_3 (R_2)	0.92

In parallel, analogs were evaluated for their mechanism of action through cell wall viability and protein inhibition assays. For the deprotected analogs, all were evaluated except the amine and R1 chlorine analogs. For the protected analogs, only the chlorine analogs in positions R_2 and R_4 and the methyl analog were evaluated. Three of the protected substituted analogs; bromine, R_2 chlorine, and methyl, exhibited activity early in the assay with cell growth recovery occurring thereafter as shown in Figure 10a and b. The bromine inhibited from 2 to 12 hours and chlorine and methyl only for 2 to 8 hours. While activity was not significant enough to be observed at lower concentrations used in the cell death assays, results indicate that some disruption is occurring in the cell wall as a result of substitutions to empetroxepin ring C. Bromine may have a slightly stronger effect than either methyl or chlorine. No activity was observed in the protein inhibition assays, indicating protected analogs are not acting on proteins.

As expected, based on results of the cell death assays, all three deprotected analogs showed inhibition of the cell wall against *S. aureus* as shown in Figure 10c. It was noted, however, that the positive control, vancomycin, did not inhibit and thus the assay must be performed again to verify results. Surprisingly, all three deprotected analogs showed significant cell wall inhibition against *E. coli* as shown in Figure 10d, although cell death activity was not observed. While cell wall inhibition assays are conducted at five times the highest concentration of cell death assays, the significance of inhibition suggests that some cell death activity should have been detected. It was noted during the cell death assays that significant discoloration of the plate well occurred during incubation, which can sometimes obscure results at the higher concentrations due to interference with absorbance readings at 590 nm. A rerun of the cell death assay with absorbance at an alternate wavelength may prove beneficial in resolving these results as antibiotics that exhibit broad spectrum activity are rare. As shown in Figure 10f, gram negative bacteria are surrounded by an additional lipopolysaccharide membrane which make them particularly difficult to penetrate.

Finally, the adjustment of chlorine from R_2 to R_4 significantly increases cell wall inhibition to levels exhibited by the positive control as shown in Figure 10e. No protein inhibition activity was observed for any protected analogs. Collectively, these results suggest that antibacterial activity of empetroxepin yields from ring A but can be increased through substitutions to the C ring.

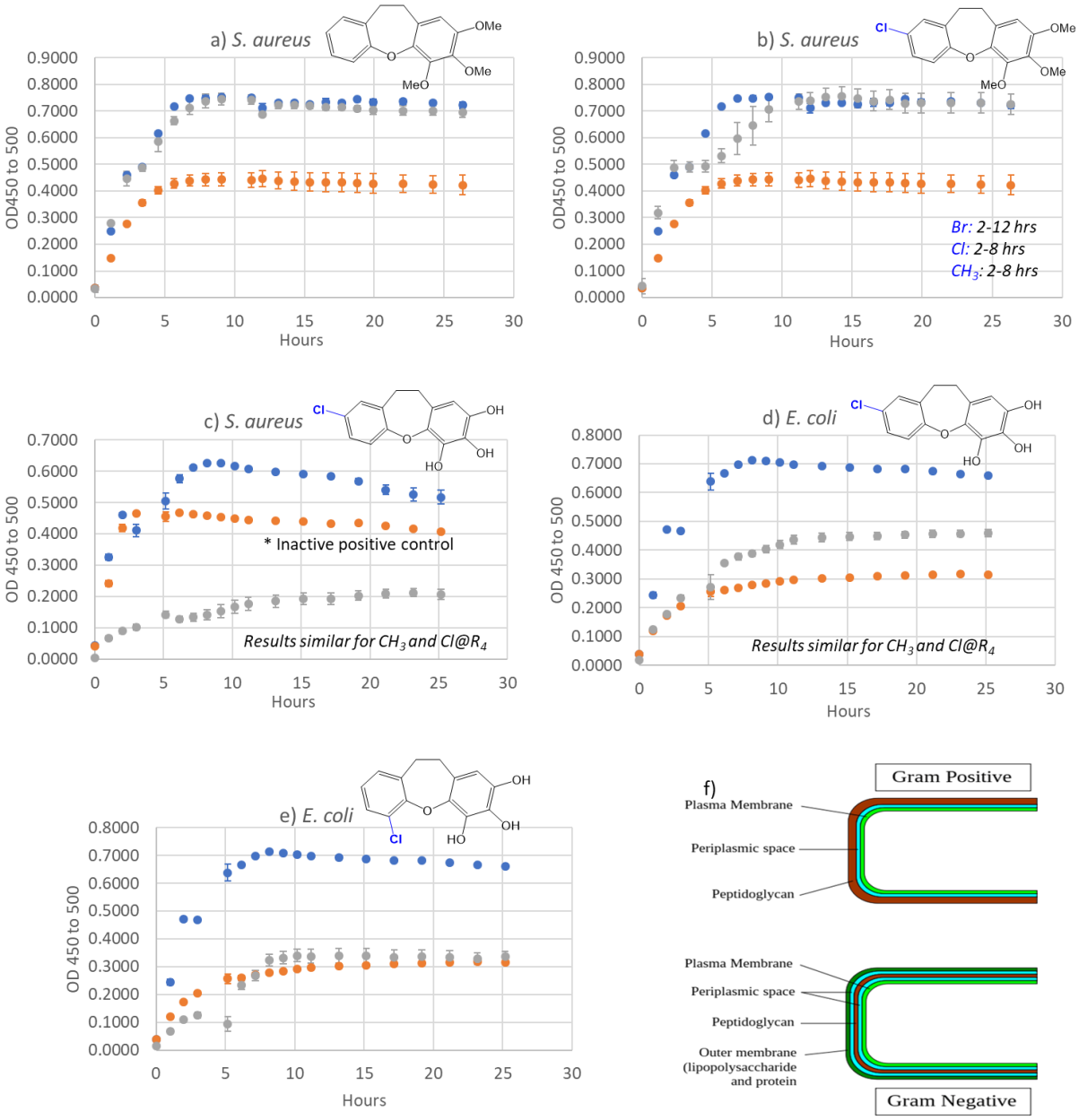

All mechanism of action data collected by Lauren Fields, UNCA

Figure 10. (a-e) Molecular structures and results of cell wall inhibition assays. Grey circles indicate analog activity, orange the positive control, and the negative control in blue. Horizontal markers indicate standard deviations. (f) Graphic illustration comparing the composition of Gram-negative versus Gram-positive cell walls.

3. Conclusions

A complete strategy to synthesize empetroxepin analogs was proposed and increased yields over a prior proposal from negligible to 8% overall. Out of thirteen attempted analogs, eight protected and five deprotected analogs were achieved in enough quantity to characterize via ^{1}H NMR, ^{13}C NMR, and IR spectroscopy. Each successful analog was subjected to cell death, cell wall inhibition, and protein inhibition assays on both a Gram-negative (*E. Coli*) and Gram-positive (*S. Aureus*) bacteria.

Deprotected analogs showed antibacterial activity against *S. aureus* between 0.46 and 0.92 mg/mL but no activity against *E. coli*. However, cell wall inhibition assays suggested broad spectrum activity with the R_4 chlorine deprotected analog yielding the highest activity and comparable to the positive control vancomycin. This research demonstrated that empetroxepin antibacterial activity is a function of ring A, but that activity can be adjusted through substitution on ring C, particularly at position R_4 with a chlorine atom. The mechanism of action is through cell wall inhibition and not via protein inhibition.

4. Experimental Methodology

^1H and ^{13}C spectra were obtained using $CDCl_3$ as the solvent on a Varian Gemini 2000 with an Oxford Instruments 400 MHz superconducting magnet. The ^1H and ^{13}C NMR chemical shifts were referenced to either the solvent peak for $CDCl_3$ at δ_H 7.27 and δ_C 77.23 or where noted to DMSO at δ_H 2.5 and δ_C 77.23.

IR: All spectra were obtained using a Thermo Scientific NICOLET iS10 scanner.

LCMS: All spectra were obtained using CH_3OH/H_2O with 1% acetic acid as the solvent on Shimadzu LCMS-2020.

Antibacterial Assays: Absorbance values were obtained with the BioTek Synergy HTX multi-mode 96 well plate reader and Gen5 2.09 software with Standard S. Aureus Assay Protocol_no blanks.prt protocol. Wavelengths are indicated below for the individual assays.

Chemical Reagents: All solvents and reagents were obtained from commercial suppliers and used without further purification with the exception to NBS and AIBN which were recrystallized before use. Additional care was used when handling dichloromethane due to its carcinogenic properties. Additional care was used when handling trichlorosilane due to potential spontaneous combustion when exposed with air.

Biological Reagents: Bacterial strains used were *Staphylococcus aureus* (ATCC 29213) and *Escheria coli* (ATCC 15022). The following purchased materials are listed: full-strength tryptic soy broth (FS TSB) (BD Difco), DMSO (VWR), 96 well clear round-bottom plate (Thermo Fisher), XTT salt (Sigma-Aldrich), vancomycin (VWR), amoxycillin (Thermo Fisher), MOPS solid (Thermo Fisher), sodium sulfate (VWR), ethylenediaminetetraacetic acid (EDTA) (JT Baker), carbonic anhydrase (Krackeler Scientific), 4-nitrophenyl acetate (4-NPA) (Fisher), 96 well flat-bottom plate (Falcon).

Reaction 1: EAS Bromination: 2-Bromo-3,4,5-Trimethoxy toluene (2): 3,4,5-Trimethoxy toluene **(1)** (10 g, 55 mmol, 1 eq) was added to a flame dried 1000 mL round bottom flask with stir bar containing anhydrous acetonitrile (484 mL, 0.113 M) under an argon atmosphere. The mixture was cooled to 0 °C. While stirring at 0 °C, NBS (10.74 g, 60.3 mmol, 1.1eq) was added in 7 portions (~3 g each) at 10 min intervals. The reaction mixture was then allowed to warm to room temperature for an additional 10 minutes. The reaction mixture was diluted with EtOAc (~500 mL) and washed with DI water (2 x 500 mL), saturated aqueous NaCl (1 x 500 mL), and dried over Na_2SO_4. The EtOAc was evaporated under reduced pressure, and the crude product was purified by column chromatography (SiO_2, EtOAc-hexane, 1:19) to give 10.62 g (74 % yield) of the title compound **2** as a highly viscous colorless liquid. IR: ῡmax 3747, 2849, 2187, 2035, 1679, 1591, 1474, 1408, 1385, 1297, 1266, 1252, 1179, 1117, 918, 843, 828, 765, 719, 693 cm-1. ^1H NMR: δ 2.347 (s, 3H), 3.822 (s, 3H), 3.840 (s, 3H), 3.870 (s, 3H), 6.586 (s, 1H). ^{13}C NMR: δ 23.234, 56.034, 60.863, 61.107, 109.436, 110.764, 133.388, 140.978, 150.764, 152.229.

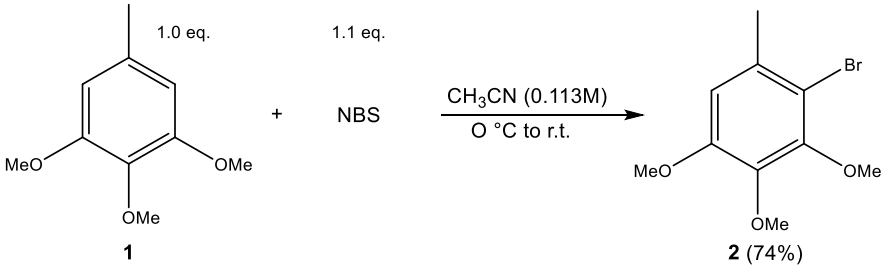

1 **2** (74%)

Reaction 2: Radical Benzylic Bromination: 2-bromo-1-(bromomethyl)-3,4,5-trimethoxybenzene (3): Compound **2** (16.5 g, 63 mmol, 1eq) was added to a 500 mL flame dried round bottom flask with a stir bar and column condenser containing CCl_4 (198 mL, 0.32M) under argon. NBS (12.4 g, 69.6 mmol, 1.1 eq) and AIBN (1.0 g, 6.3 mmol, 0.1 eq), both recrystallized, were added together to the reaction flask at the joint, turning the reaction mixture opaque light yellow. The mixture was placed in an oil bath at 80 °C under reflux for ~4 hours, during which the mixture turned orange (t = 15 min) then back to pale yellow (t = 20 min). The reaction mixture was moved to a separation funnel and washed twice with a saturated aqueous sodium thiosulfate solution. The aqueous solution was extracted three times with DCM, and the combined organic layers were washed with saturated aqueous NaCl, dried over magnesium sulfate, and filtered. The crude product was concentrated under reduced pressure revealing an orange oil. TLC revealed a mixed product which was then purified via column chromatography (SiO_2, 10% EtOAc-hexane) to give 16.0 g (75% yield) of 2- bromo-1-(bromomethyl)-3,4,5-trimethoxybenzene **(3)** as a white solid. IR: ῡmax 3001, 2978, 2940, 2832, 1567, 1482, 1451 1426, 1395, 1250, 1205, 1167, 1100, 1042, 1004, 929, 896, 805 cm-1. ^{1}H-NMR: δ 3.854 (s, 3H), 3.871 (s, 3H), 3.879 (s, 3H), 4.584 (s, 2H), 6.795 (s, 1H). ^{13}C-NMR: δ 34.173, 57.234, 61.031, 61.137, 109.658, 111.199, 132.206, 143.381, 151.275, 152.755.

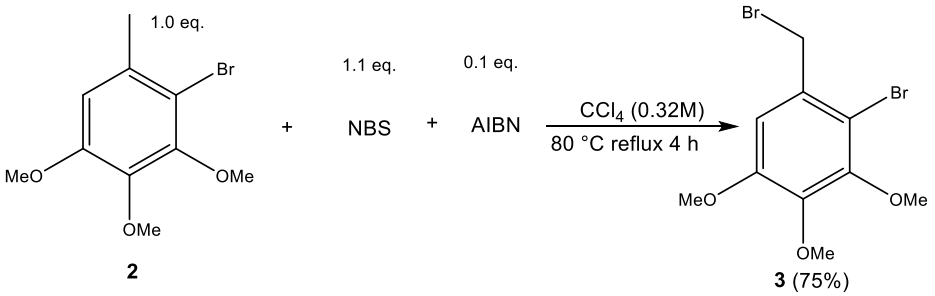

Reaction 3: Formation of the Triphenylphosphate Salt (4): 2-bromo-1-(bromomethyl)-3,4,5-trimethoxybenzene **(3)** (3.5 g, 10.3 mmol, 1.0 eq) was added to a 10 mL flame dried round bottom flask with stir bar under argon. Anhydrous DMF (5.2 mL, 2M) was added to the reaction flask via syringe followed by PPh_3 (2.7 g, 10.3 mmol, 1.0 eq) turning the reaction mixture an opaque pale yellow. The reaction mixture was stirred at room temperature for ~18 hours turning an opaque white after 20 min. ~16 mL of toluene was added to the reaction mixture and the chalky white precipitate was filtered using a fritted funnel. The precipitate was dissolved in a minimal amount of DCM. The solution was precipitated again with diethyl ether and the suspension was filtered with a fritted funnel giving 4.7 g (87% yield) of compound **4** as a white powdery solid.IR: ῡmax 3020, 2968, 2942, 2874, 1588 1568, 1484, 1435, 1393, 1341, 1250, 1206, 1105, 999, 846, 748, 724, 689 cm-1. ^{1}H NMR: δ 3.612 (s, 3H), 3.723 (s, 3H), 3.851 (s, 3H), 5.631 (s, 1H), 5.665(s, 1H), 7.175-7.182 (d, 1H, J = 2.8 Hz), 7.626-7.829 (m, 15H). ^{13}C NMR: δ 30.521, 56.463, 60.880, 61.216, 61.238, 112.375, 112.421, 113.642, 113.710, 116.937, 117.791, 122.276, 122.368, 130.072, 130.202, 134.397, 134.496, 135.137, 135.167, 143.237, 143.283, 150.835, 150.873, 152.864, 152.902.

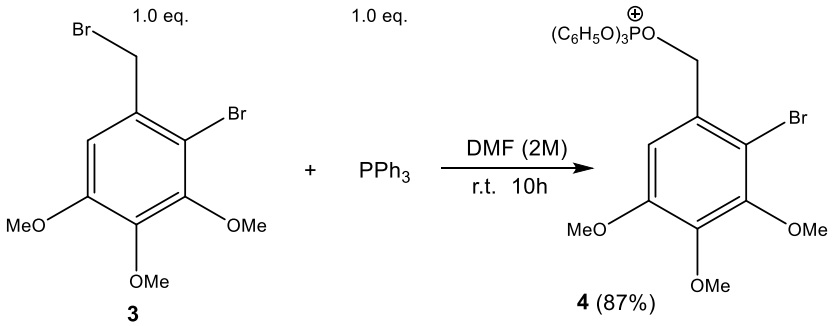

General Reaction 4: TMS Protected Alcohol (5): 5-chloro salicylaldehyde (0.5 g, 3.2 mmol, 1eq) was added to a 50 mL round bottom flask with stir bar containing anhydrous DCM (32 mL, 0.1M) under argon. The reaction was cooled to 0 °C. Anhydrous pyridine (0.643 mL, 7.9 mmol, 2.5 eq) and TMS-Cl (0.85 mL, 6.7 mmol, 2.1 eq) were then added to the reaction flask via syringe and stirred for 29 hours. The reaction mixture was washed three times with deionized water and the combined organic layers were washed with saturated aqueous NaCl, dried over sodium sulfate,

and concentrated under decreased pressure to give 0.4 g of a brown crystalline solid. NOTE: In conditions of high atmospheric moisture, TMS protected compounds are quickly decomposed. It is recommended to only condense in Vacuo. Alcohol TMS protected 5-chloro-salicylaldehyde experiences significant decomposition even in Vacuo so it is recommended to leave in solution after separation if possible. ^{1}H NMR revealed the product was a 0.09:98 ratio of compound **5** (99.9%) to 5 chloro salicylaldehyde. Product aromatic hydrogens could not be delineated from starting material so are included in the ^{1}H NMR spectra. IR: ṽmax 3234, 2874, 1682, 1660, 1568, 1473, 1378, 1273, 1156, 1128, 1082, 924, 905, 887, 832, 769, 722 cm-1. ^{1}H NMR: δ 6.590-6.613 (m, 1H), 7.104-7.158 (m, 1H), 7.462-7.469 (d, 1H), 10.059 (s, 1H). ^{13}C-NMR: δ 121.832, 126.980, 127.644, 127.865, 135.196, 156.805, 188.529.

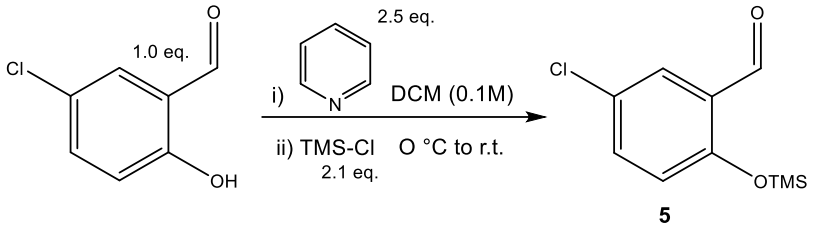

5

General Reaction 5: Wittig Olefination (6): Compound **4** (0.1.9 g, 1.24 mmol, 1.2 eq) and anhydrous DCM (15.5 mL, 0.2M) were added to a 50 mL, flame dried round bottom flask with stir bar under Argon and the reaction was cooled to 0 °C. KOtBu (0.53 g, 4.34 mmol, 1.4 eq) was added to the reaction flask turning the white mixture from bright yellow to bright red-orange. The mixture was stirred at 0 °C for 1 hr. Compound **5** (0.7 g, 3.1 mmol, 1 eq) was then added at to the reaction flask via syringe turning the mixture back to bright yellow. The reaction was warmed to room temperature and stirred for 24 h. Deionized water was slowly added to the flask to dilute the reaction mixture which was then extracted with EtOAc (3x). The combined organic layers were washed with saturated aqueous NaCl, dried over sodium sulfate, and concentrated under reduced pressure to give a white gel. The crude product was then purified via column chromatography (SiO_2, 10% EtOAc-hexanes) to give 0.1.5 g (91% yield) of a yellow viscous liquid consisting of the combined cis (36%) and trans (64%) isomers of compound **6**. IR: ṽmax 3058, 2936, 1734, 1557, 1480, 1438, 1423, 1391, 1347, 1120, 1071, 1327, 1278, 1265, 1244, 1166, 1047, 1008, 909, 818, 724, 695 cm^{-1}. Cis: ^{1}H NMR: δ 3.437 (s, 3H), 3.875 (s, 3H), 3.905 (s, 3H), 6.533(s 1H), 6.641-6.672 (d 1H), 6.756-6.763 (m, 4H, J=12 Hz). Trans: ^{1}H NMR: δ 3.875 (s, 3H), 3.905 (s, 6H), 7.000 (s, 1H), 7.022-7.069 (m 2H), 7.165-7.205 (d 1H, J=16 Hz), 7.420-7.461 (d, 1H, J=16 Hz), 7.52 (s, 1H). ^{13}C NMR: δ 14.129, 21.169, 55.731, 56.135, 61.063, 61.093, 61.261, 61.314, 105.388, 109.110, 110.689, 111.154, 117.028, 117.203, 124.419, 124.671, 124.869,125.426, 125.922, 126.540, 128.500, 128.653, 128.882, 129.248, 131.666, 133.069, 142.627, 150.613, 150.689, 152.009, 152.032, 152,497, 152.589, 172.513.

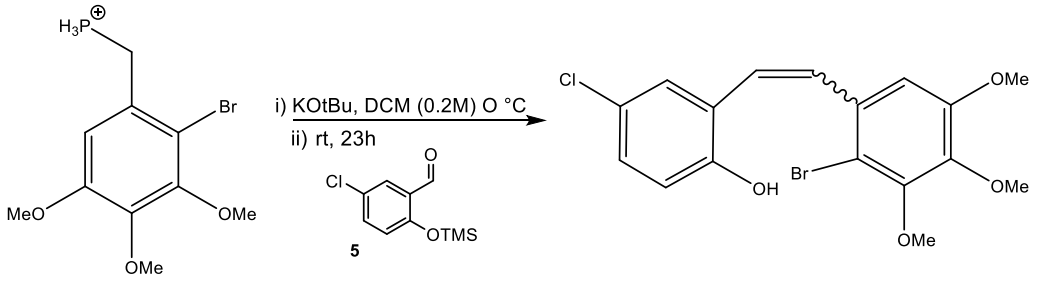

4 **5** **6** (91%)

General Reaction 6: Hydrogenation of Cis and Trans Isomers (7): Compound **6** (1.2 g, 3.0 mmol, 1 eq) was dissolved in ethanol (28 mL, 0.11 M) and then added at the joint via syringe to a 100 mL flame dried round bottom flask with stir bar and column condenser under Argon. NaOAc (1.23 g, 15 mmol, 5 eq) and p-toluene sulfonylhydrazide (1.12 g, 6 mmol, 2 eq) were then added at the joint and refluxed overnight at 120 ºC. Once cool, the reaction was poured into a separation funnel containing saturated aqueous $NaHCO_3$ and washed 2X with Et_2O. The organic layers combined and washed with brine and dried over Na_2SO_4. The solvent was removed in Vacuo. The residue was purified via column chromatography (SiO_2, 15% EtOAc-hexane) to give compound **7** (0.43 g, 36%) as a white solid. IR: ṽmax 3832, 3688, 3458, 3395, 3367, 2952, 2171, 1972, 1927, 1573, 1497, 1396, 1328, 1167, 1104, 1004, 910, 819, 736, 673 cm-1. ^{1}H NMR: δ 2.824-2.989 (m, 4H), 3.791 (s, 3H), 3.876 (s, 3H), 3.909 (s, 3H), 5.047 (s,

1H), 6.505 (s, 1H), 6.708-6.729 (d, 1H), 7.040-7.074 (m, 2H)^{13}C NMR: δ 30.513, 36.661, 56.104, 61.055, 61.185, 109.194, 110.392, 116.547, 125.296, 127.211, 128.912, 130.087, 136.143, 141.460, 150.850, 152.322, 152.467.

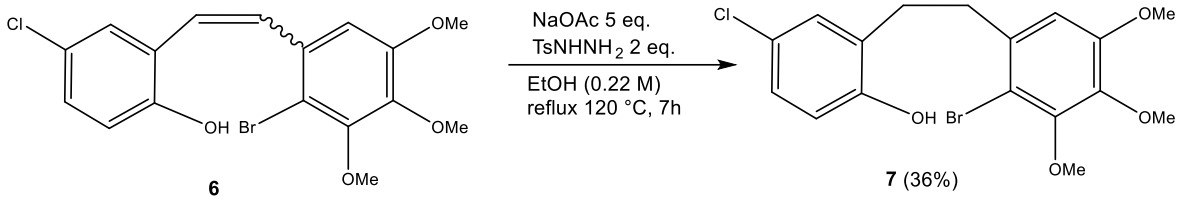

6 **7** (36%)

General Reaction 7: Etherification (8): NaH (60% in oil dispersion, 38 mg, 1.6 mmol, 1.1 eq) was added to a stirred solution of compound **10** (0.43 g, 1.1 mmol, 1 eq) and CuBr·Me_2S (99%, 0.44 g, 2.14 mmol, 2 eq) in anhydrous pyridine (3.5 mL, 0.33 M) under Argon at ambient temperature. After stirring for 15 min, the reaction mixture was heated at 120 °C for 18 h. The mixture was cooled, then poured into 1.37 M HCl and extracted 5x with DCM. The organic layer was washed with 0.31 M $CuSO_4$ and dried over sodium sulfate, and the solvent removed in Vacuo. The residue was purified via column chromatography (SiO_2, 5% EtOAc-hexane) to give compound **8** (0.23 g, 68%) as a pale yellow crystalline solid: IR: ῡmax 3469, 3359, 3113, 2935, 1587, 1469, 1559, 1224, 1193, 1121, 1084, 1043, 1028, 993, 974, 948, 865, 830, 758, 705 cm-1. ^{1}H NMR: δ 3.072 (s, 4H), 3.819 (s, 3H), 3.866 (s, 3H), 3.970 (s, 3H), 6.427(s, 1H), 7.078-7.110 (m, 2H), 7.160-7.180 (d, 1H) ^{13}C-NMR: δ 30.147, 31.116, 56.158, 61.246, 61.993, 106.913, 122.711, 127.097, 128.393, 128.569, 120.430, 132.665, 141.139, 144.625, 145.678, 149.644, 155.564.

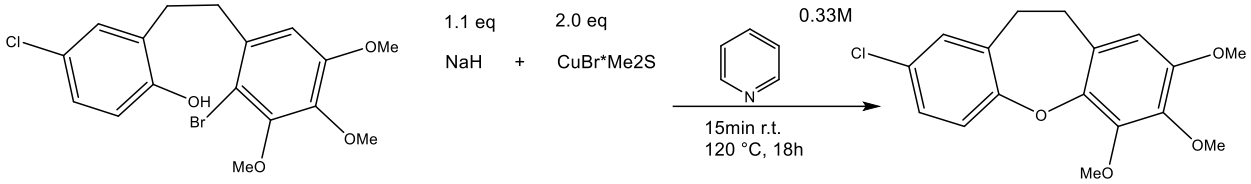

7 **8** (68%)

Reaction 8: Demethylation (9): A solution of 1M borontribromide dimethylsulfide complex in DCM (3.44 ml, 5 eq) and compound **8** (0.22 g, 0.688 mmol) was refluxed for 4 h at 40 °C. The reaction was cooled to room temperature before being carefully quenched with cold DI H_2O (5 mL) at 0 °C then stirred vigorously for 2 h. The resulting solution was extracted 3X with DCM and the material purified by column chromatography (SiO_2, 20% EtOAc-hexane) yielding the completely demethylated compound **9** (.15 g, 77%) as a light yellow solid: IR: ῡmax 3381, 2924, 2854, 1620, 1583, 1489, 1457, 1298, 1230, 1183, 1104, 1059, 972, 914, 756 cm-1. (DMSO Solvent) ^{1}H NMR: δ 2.839-2.984 (m, 4H), 6.073 (s, 1H), 7.171-7.197 (m, 2H), 7.374-7.402 (d, 1H), 8.203 (s, 1H), 8.659 (s, 2H). ^{13}C-NMR: δ 29.208, 31.306, 105.746, 122.733, 122.603, 127.801, 127.630, 130.674, 132.443, 133.923, 138.065, 138.599, 142.748, 156.295.

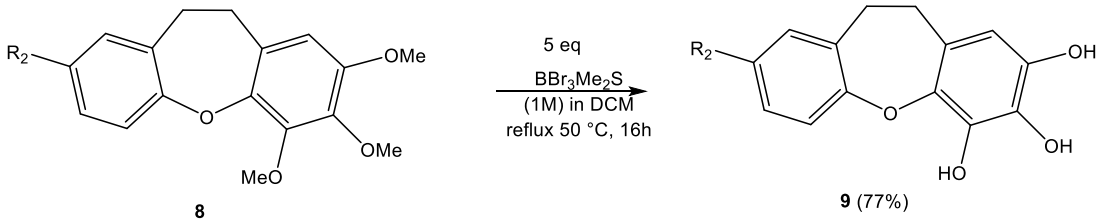

8 **9** (77%)

Antibacterial Cell Death Assay: *S. aureus* and *E. coli* were cultured in petri dishes using the streak method. Overnight bacterial cultures were prepared under sterile conditions. For each bacterial strain, cells from a single bacterial colony were seeded into a test tubes containing 10 mL of full-strength tryptic soy broth (FS TSB). A third tube was prepared containing only the FS TSB to serve as a negative control. Lids were loosely placed and then taped onto the tubes without tightening to ensure access to oxygen and agitated for 18 h at 37 ºC. On the day following, approximately 5 mg of the empetroxepin analogs were diluted in small glass vials to a final concentration of 100 mg/mL using biological grade dimethyl sulfoxide (DMSO)(VWR). A master dilution plate was prepared by adding

9 µL of DMSO to all but the top wells. To the top wells were added 10 µL of 100 mg/mL chloramphenicol (Fisher) to serve as the positive control, the appropriate diluted compound, and DMSO to serve as the negative control, all in duplicate. Compounds were diluted down each column by taking 1 µL from the top well and mixing into the well beneath, resulting in 10-fold dilutions from 100 mg/mL to 0.00001 mg/mL. One assay plate each for *S. aureus* and *E. coli* were prepared by adding 89 µL FS TSB, 10 µL of bacteria overnight culture, and 1 µL of compound from the corresponding well on the master plate. After incubating assay plates at 37 ºC for 18h, the lids were removed, and absorbance at 590 nm was collected on a Biotek Synergy HTX Multi-mode plate reader. The mean IC_{50} was determined for each analog.

Antibacterial Cell Wall Viability Assay: *S. aureus* and *E. coli* were cultured in petri dishes using the streak method. Overnight bacterial cultures were prepared under sterile conditions. For each bacterial strain, cells from a single bacterial colony were seeded into a test tubes containing 10 mL of FS TSB. A fifth tube was prepared containing only the FS TSB to serve as a negative control. Lids were loosely placed and then taped onto the tubes without tightening to ensure access to oxygen and agitated for 18 h at 37 ºC. On the day following, approximately 5 mg of the empetroxepin analogs were diluted in small glass vials to a final concentration of 100 mg/mL using biological grade DMSO. The assay was prepared with bacteria and 10% TSB. The empetroxepin analogs were introduced, and then an XTT tetrazolium salt was added for visualization. The XTT product was read every 1 hour for 10 hours and then every 2 hours until 24 hours, each at an absorbance of 450 to 500 nm. Background absorbance was read at 630 to 690 nm. Plates were read with the lid on, using a Biotek Synergy HTX Multi-mode plate reader for quantification. Analog performance was ranked against the performance of amoxicillin or vancomycin, the positive controls for Gram-negative and Gram-positive bacteria, respectively. DMSO was used as the negative control. If the analog's inhibition was not competitive with amoxicillin, but still displaying minor inhibition, it was ranked as minimally inhibitory.

Antibacterial Protein Inhibition Assay: Approximately 5 mg of the empetroxepin analogs were diluted in small glass vials to a final concentration of 100 mg/mL using biological grade DMSO. The MOPS buffers were prepared from 9.6 ml DI H2O, 50 mM MOPS, 33 mM sodium sulfate and pH adjusted to 7.5 using potassium hydroxide. To the buffer was added 1 mM EDTA and the solution stored on ice. The protein, a carbonic anhydrase solution, was prepared from 9 mL of the MOPS buffer and 29 kDa of carbonic anhydrase. A solution of 5 mM 4-NPA solution was used as the activator and consisted of 900 µL of MOPS buffer, 100 µL DMSO, and 5 mM of 4-NPA solid. The solution was kept on ice and due to the light sensitivity of 4-NPA, also kept in complete darkness. The assay was prepared in a clear 96-well flat-bottom plate and kept on ice during pipetting. Each antibiotic was assayed in quadruplicate (n=4) with acetazolamide as the positive control and DMSO as the negative control. Into each well was added 100 µL carbonic anhydrase solution and 1 µL antibiotic, and the plate incubated for 15 minutes at 37 ºC. After 15 minutes was added 10 µL of the 4-NPA solution and absorbance values collected immediately at 490 nm every 15 seconds for 5 minutes.

5. Acknowledgements

The author would like to thank Dr. Amanda Wolfe for all her guidance, the Wolfe Research Team for their contributions and support, and the University of North Carolina Asheville Chemistry Department for all their expertise and advice. Thank you to Lauren Fields for her extensive data collection. Thank you to the Research Corporation - Cottrell Scholars Award and the Office of Undergraduate Research for their generous financial support.

6. References

1. World Health Organization (WHO). Global Strategy for Containment of Antimicrobial Resistance, Geneva (**2001**).
2. O'Neill, J., Tackling Drug-Resistant Infections Globally: Final Report and Recommendations. *Rev. Antimicrob. Resist*. **2016**. (Accessed on 11 April, 2018). https://amr-review.org/.
3. Boucher, H; et al. An Update from the Infectious Diseases Society of America. *Clin. Infect. Dis.*, **2009**, *28*, 1-12.
4. Singh, S. B. Confronting the challenges of discovery of novel antibacterial agents. *Bioorg. Med. Chem. Lett.* **2014**, *24*, 3683-3689.

5. Brown, D. G.; Lister, T.; May-Dracka, T. L. New natural products as new leads for antibacterial drug discovery. *Bioorg. Med. Chem. Lett.* **2014**, *24*, 413-418.
6. World Health Organization (WHO). Antimicrobial Resistance: Global Report On Surveillance, Geneva (**2014**).
7. Stadler, A., Dersch, P. How to Overcome the Antibiotic Crisis Facts, Challenges, Technologies and Future Perspective. *In Current Topics in Microbiology and Immunology.* Springer International Publishing AG **2016**; Vol. 398; p 3. World Health Organization (WHO). World Malaria Report (**2016**).
8. Bouthillett, L.M., Darcey, C.A., Handy, T.E., Seaton, S.C., Wolfe, A.L. Isolation of the Antibiotic Pseudopyronine B and SAR Evaluation of C3/C6 Alkyl Analogs. *Bioorg. Med. Chem. Lett*. **2014**, 27(12), 2762-2765.
9. Li, H.; Jean, S.; Webster, D.; et al. Dibenz[b,f]oxepin and Antimycobacterial Chalcone Constituents of *Empetrum nigrum*. *J. Nat. Prod.* **2015**, *78(11)*, 2837-40.
10. Boonphong S., Puangsombat P., Baramee, A., Mahidol C., Ruchirawat S., Kittakoop, P. Bioactive Compounds from *Bauhinia purpurea* Possessing Antimalarial, Antimycobacterial, Antifungal, Anti-inflammatory, and Cytotoxic Activities. *J. Nat. Prod.* **2007**, 70, 795-801.
11. He, C., Preiss, L., Wang, B., Fu, L., Wen, H., Zhang, X., Cui, H., Meier, T., Yin, D. Structural Simplification of Bedaquiline: the Discovery of 3-(4-(N,N-Dimethylaminomethyl) phenyl)quinoline-Derived Antitubercular Lead Compounds. *Chem. Med. Chem.* **2016**, 11, 1 – 15.
12. Niu, S., Liu, D., Hu, X., Proksch, P., Shao, Z., Lin, W. Spiromastixones A−O, Antibacterial Chlorodepsidones from a Deep-Sea-Derived Spiromastix sp. Fungus. *J. Nat. Prod.* **2014**, 77, 1021−1030.
13. Lin, J., Zhang, W., Jiang, N., Niu, Z., Bao, K., Zhang, L., Liu, D., Pan, C., and Yao, X.. Total Synthesis of Bulbophylol-B. *J. Nat. Prod.* **2008**, 71, 1938–1941.

7. Figures

1. Reprinted from WHO. Antimicrobial Resistance: Global Report On Surveillance, Geneva (**2014**). Graphic used in accordance with the terms of the United Kingdom Creative Commons Attribution 4.0 International Public License.

2. Reprinted from L.L. Silver, Challenges of Antibacterial Discovery, Clinical Microbiology Reviews 2011, 24 (1) 71-109. Graphic used with permission of the American Society for Microbiology, Copyright © 2011.

3. Reprinted from Trends in Microbiology, 22:4, T.F. Schäberle and I.M. Hack, Overcoming the current deadlock in antibiotic research, 165-167, Copyright 2014 with permission from Elsevier.

6. Reprinted with permission from the Journal of Natural Products, Bioactive Compounds from Bauhinia purpurea Possessing Antimalarial, Antimycobacterial, Antifungal, Anti-inflammatory, and Cytotoxic Activities,Surat Boonphong, Pakawan Puangsombat, Apiwat Baramee, Chulabhorn Mahidol, Somsak Ruchirawat,and Prasat Kittakoop, **2007** *70* (5), 795-801. Copyright 2007 American Chemical Society